

# Probing the diamagnetic term in light-matter interaction

Matteo A. C. Rossi,<sup>1,2</sup> Matteo Bina,<sup>1</sup> Matteo G. A. Paris,<sup>1,3</sup> Marco G. Genoni,<sup>1,4</sup> Gerardo Adesso,<sup>2</sup> and Tommaso Tufarelli<sup>2</sup>

<sup>1</sup>Quantum Technology Lab, Dipartimento di Fisica, Università degli Studi di Milano, 20133 Milano, Italy

<sup>2</sup>School of Mathematical Sciences, The University of Nottingham, Nottingham NG7 2RD, United Kingdom

<sup>3</sup>INFN, Sezione di Milano, I-20133 Milano, Italy

<sup>4</sup>Department of Physics and Astronomy, University College London, London WC1E 6BT, United Kingdom

(Dated: March 10, 2022)

Should the Dicke model of light-matter interaction include a diamagnetic term? This question has generated intense debate in the literature, and is particularly relevant in the modern contexts of cavity and circuit quantum electrodynamics. We design an appropriate probing strategy to address the issue experimentally. Applying the tools of quantum estimation theory to a general Dicke model, we quantify how much information about the diamagnetic term (or lack thereof) is contained in the ground state of the coupled system. We demonstrate that feasible measurements, such as homodyne detection or photon counting, give access to a significant fraction of such information. These measurements could be performed by suddenly switching off the light-matter coupling, and collecting the radiation that naturally leaks out of the system. We further show that, should the model admit a critical point, both measurements would become asymptotically optimal in its vicinity. We finally discuss binary discrimination strategies between the two most debated hypotheses involving the diamagnetic term.

*Introduction.* The ultra-strong coupling (USC) regime of light-matter interaction has recently attracted much interest, thanks to impressive advances in theory and experiments [1, 2]. A number of interesting phenomena, of fundamental physical appeal and potential impact on future quantum technologies, arise in this regime, including the formation of a nontrivial ground state [3], dynamical Casimir-like effects [4], and the possibility of quantum phase transitions [5, 6].

The USC regime is entered when the light-matter coupling constant, say  $\lambda$ , is so large that the rotating-wave approximation breaks down: in this situation one is no longer able to neglect the so-called “counter-rotating terms” in the minimal coupling Hamiltonian [7]. While this brings about exciting new physics, it results also in formidable computational challenges. Effective models featuring a small number of degrees-of-freedom, such as the Dicke Hamiltonian [5], are extremely useful in this context: they can reveal crucial features of the new regime while keeping computations tractable. However, there is disagreement in the literature regarding the specific form that these few-degrees-of-freedom models should take, in particular concerning the presence (or otherwise) of the so-called diamagnetic or  $A^2$  term. Many authors include this term in their effective models and stress its importance in preventing the Dicke phase transition [8–11] and in limiting the effectively achievable light-matter coupling [12]. In contrast, other authors hold that the  $A^2$  term can be eliminated when an accurate, few-mode approximation is carried out [13–15]. Ref. [5] showed that the term must be present in effective models of cavity quantum electrodynamics (QED), and that the associated coupling constant should be constrained by the Thomas-Reiche-Kuhn (TRK) sum rule. On the other hand, the same authors maintain that the term can be avoided in circuit QED [5], a claim which has generated further debate [16–18].

In this Letter we take the view that the minimal coupling Hamiltonian, underlying all the effective USC models discussed in the literature, is too complex to be fully understood with the currently available theoretical and computa-

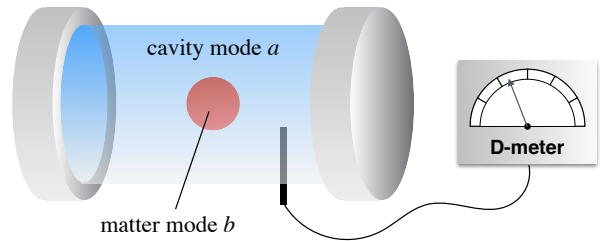


FIG. 1. The parameter  $D$ , quantifying the strength the diamagnetic term in the Dicke Hamiltonian (1), may be estimated experimentally by performing an appropriate measurement on the coupled light-matter system. Our results suggest that realistic measurements such as homodyne detection or photon counting of the cavity field  $a$  are well suited to this task in a broad range of the model parameters.

tional tools. We thus take a complementary approach to the  $A^2$ -term debate, and instead of trying to address the question theoretically from first principles, we propose that it may be settled experimentally via an appropriate measurement. Steps in this direction have been taken in a multimode circuit QED setting [19], however we are the first to apply the tools of quantum metrology to the issue, setting a theoretical benchmark for any future experiment.

We consider a general Dicke model of two coupled oscillators featuring counter-rotating terms and an  $A^2$ -like term with unknown coupling constant  $D$ . As the establishment of a nontrivial ground state is perhaps the simplest signature of the USC, we find it natural to ask how much information about  $D$  is contained in this state, and how much of it can be extracted by realistic measurements (see Fig. 1 for an illustration). Exploiting the tools of quantum estimation theory [20–25], we are able to give sharp quantitative answers to these questions.

Besides deriving the ultimate bounds on the estimation precision of  $D$ , we find that feasible measurements, such as homodyne detection or photon counting, allow for the extraction of a significant fraction of the available information. Namely, homodyne detection is optimal for vanishing  $\lambda$ , still provid-

ing a close-to-optimal performance for  $\lambda$  between 10% and 20% of the mode frequencies. This regime of relatively small coupling (yet within the USC) is relevant in both cavity QED [26] and circuit QED experiments [27, 28]. While we tackle the problem in its full generality, we also obtain compact analytical results for three important limiting cases: (i)  $D \simeq 0$ ; (ii)  $D \simeq D_{\text{TRK}}$ , where  $D_{\text{TRK}}$  is the value derived from the TRK sum rule [5, 29]; (iii)  $D \simeq D_{\text{crit}}$ , where  $D_{\text{crit}}$  is the threshold for the Dicke phase transition. In case the model admits a phase transition, we further find that the considered measurements become approximately optimal near the critical point.

We complement our analysis by discussing the problem of binary discrimination [30, 31] between  $D = 0$  and  $D = D_{\text{TRK}}$ , which may be relevant in circuit QED, where the choice is between a TRK value [16] or a negligible value [5]. We conclude with an outlook on possible directions for the experimental realization of the proposed estimation and discrimination schemes.

*The model.* Let us start by introducing the Hamiltonian of the system. We denote with  $a$  the photonic cavity mode, of bare frequency  $\omega_a$ , and with  $b$  the matter mode, with frequency  $\omega_b$ . After setting  $\hbar = 1$ , the Hamiltonian reads

$$\mathcal{H} = \omega_a a^\dagger a + \omega_b b^\dagger b + \lambda(a + a^\dagger)(b + b^\dagger) + D(a + a^\dagger)^2, \quad (1)$$

where  $\lambda$  is the light-matter coupling strength and the last is the diamagnetic term, with the constant  $D$  being the object of our discussion. Being quadratic in the field operators,  $\mathcal{H}$  is diagonalizable [29] and can be written, up to an irrelevant constant, as  $\mathcal{H} = \omega_U p_U^\dagger p_U + \omega_L p_L^\dagger p_L$ , where  $p_{U,L}$  are bosonic operators for the upper and lower polaritonic modes. The eigenfrequencies  $\omega_{U,L}$  are reported in [29]. For the frequencies to be real, the model parameters must satisfy the inequality

$$D \geq D_{\text{crit}} \equiv \lambda^2/\omega_b - \omega_a/4. \quad (2)$$

If the diamagnetic term is absent, i.e. we set  $D = 0$  in Eq. (1), we recover the standard Dicke Hamiltonian, with a quantum phase transition at  $\lambda = \lambda_{\text{crit}} \equiv \sqrt{\omega_a \omega_b}/2$ . On the other hand, if the diamagnetic term is included and we impose that the Hamiltonian satisfies the TRK sum rule,

$$D = D_{\text{TRK}} \equiv \lambda^2/\omega_b, \quad (3)$$

then Eq. (2) is always satisfied and the phase transition is suppressed. The ground state of the Hamiltonian is the vacuum state of the polaritonic modes, i.e. a Gaussian state with zero mean and covariance matrix  $\sigma_0 = \mathbb{I}/2$ . Expressing this state in terms of the initial modes  $a$  and  $b$ , we obtain a non-trivial, two-mode squeezed Gaussian state with covariance matrix  $\sigma = S \sigma_0 S^T$ , where the suitable symplectic transformation  $S$  [29] is reported in the Supplemental Material (SM) [32].

*Quantum estimation methods.* Let us now address the problem of estimating  $D$ , and in doing so we shall review the basics of quantum estimation theory. In order to determine the value of the unknown parameter, one collects measurement outcomes from experiments and builds an estimator  $\hat{D}$ , i.e. a function of the data that will return our best

guess for the value of  $D$ . Assuming that the estimator is unbiased, its precision, in the limit of a large number  $n$  of measurements, is bounded from below by the Cramér-Rao bound [33]  $\text{Var} \hat{D} \geq [nF(D)]^{-1}$ , where  $F(D)$  is the Fisher information (FI) of the probability distribution  $p(x|D)$ , defined as  $F(D) = \int dx p(x|D) [\partial_D \ln p(x|D)]^2$ . Here  $p(x|D)$  is the conditional probability that the outcome of the measurement is  $x$ , if the parameter value is  $D$ . If we define the quantum Fisher information (QFI)  $H(D)$  as the supremum of the Fisher information over all possible quantum measurements described by positive operator-valued measures (POVMs), we obtain the quantum Cramér-Rao bound, i.e. the ultimate lower bound on the achievable precision in the estimation of  $D$  [25].

The QFI with respect to  $D$  can be evaluated analytically for Gaussian states [34–36] and for the case at hand is given by

$$H(D) = \text{Tr}[\Omega^T \partial \sigma \Omega \Phi] \quad (4)$$

where  $\partial$  denotes the derivative with respect to  $D$ ,  $\Omega = \oplus_{i=1}^2 \begin{pmatrix} 0 & 1 \\ -1 & 0 \end{pmatrix}$  is the symplectic matrix, and the matrix  $\Phi$  satisfies the linear equation  $\partial \sigma = 2\sigma \Omega \Phi \Omega^T \sigma - \frac{1}{2} \Phi$ . The expression for the QFI is too cumbersome to be reported in this Letter, thus we report it in the SM [32], but in the following we discuss its behavior in the cases of interest for our discussion. We also note that the QFI is a homogeneous function of the parameters of the Hamiltonian:  $H(\alpha D, \alpha \omega_a, \alpha \omega_b, \alpha \lambda) = \alpha^{-2} H(D, \omega_a, \omega_b, \lambda)$ .

The QFI for the two-mode ground state is a relevant benchmark for the precision of any measurement on the system. Feasible experiments, however, will typically involve the measurement of only one of the modes, mainly the photonic mode  $a$ . It is thus interesting to evaluate also the QFI  $H_a(D)$  for the reduced state of the mode  $a$ , which is a squeezed thermal state [32].

Homodyne detection corresponds to the measurement of the quadrature operator  $\hat{x}(\phi) = (ae^{-i\phi} + a^\dagger e^{i\phi})/\sqrt{2}$ , where  $\phi$  is an arbitrary angle. For the reduced state  $\rho_a$ , the probability distribution for the outcome of  $x(\phi)$  is a normal distribution with zero mean and covariance  $\sigma_{11} \cos^2 \phi + \sigma_{22} \sin^2 \phi$ ; the corresponding FI,  $F^{(\text{hd})}$  is reported in the SM [32]. It is further argued that the FI has a maximum at  $\phi = 0$ : this has the important consequence that the best measurement angle does not depend on the (yet unknown)  $D$  parameter. On the other hand, the FI for photon counting cannot be determined analytically as it involves an infinite sum of the terms  $p(n) = \langle n | \rho | n \rangle$ , i.e. the probabilities of finding a photon in the Fock state  $|n\rangle$  [36, 37]; we evaluate it numerically in a truncated Fock space.

*Results: Probing the diamagnetic term.* Let us start by focusing on the regime of relatively small coupling within the USC. The QFI has a non vanishing limiting value

$$H(D) = \frac{2}{(4D + \omega_a)^2} + O(\lambda^2), \quad (5)$$

which shows how, in this regime, smaller values of  $D$  can be estimated more efficiently, but, on the other hand, a large number of measurements is needed in order to *neutralize* the contribution given by the mode frequency  $\omega_a$  and obtain a precise

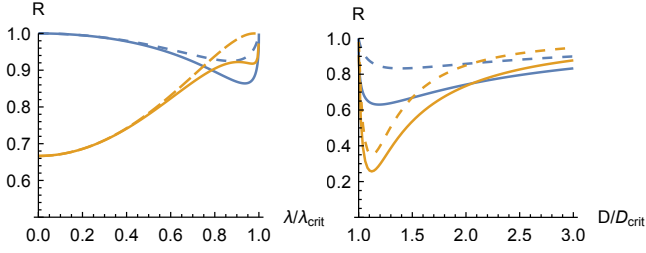


FIG. 2. Left: Ratio  $R$  between the FI and the QFI for the two modes (solid) and the photon mode (dashed) for  $D = 0$  as functions of  $\lambda$ . Homodyne detection is highlighted in blue and photon counting in orange. The plot is obtained for  $\omega_a = \omega_b = \lambda = 1$ . Homodyne detection is optimal for small  $\lambda$  and both measurements saturate the QFI when  $\lambda$  is close to  $\lambda_{\text{crit}}$ . Right: Plot of the same quantities when  $D$  gets close to the critical value  $D_{\text{crit}}$ . Both measurements saturate the QFI in the limit  $D \rightarrow D_{\text{crit}}$  and  $D/D_{\text{crit}} \rightarrow \infty$ , with homodyne detection reaching generally higher ratios in the region close to the critical value.

estimation. Remarkably, the FI for the homodyne measurement saturates  $H(D)$  up to second order in  $\lambda$ , indicating that, no matter what the true value of  $D$  is, we can extract all the available information by measuring the quadrature of the cavity mode  $a$  when  $\lambda$  is sufficiently small. In detail, if we consider the plausible scenario  $D \lesssim D_{\text{TRK}}$ , the ratio between FI and  $H(D)$  reads

$$\frac{F^{(\text{hd})}(D \lesssim D_{\text{TRK}})}{H(D \lesssim D_{\text{TRK}})} = 1 - \frac{8\omega_a^2}{(\omega_a + \omega_b)^4} \lambda^2 + O(\lambda^4). \quad (6)$$

We can now investigate the estimation properties of the diamagnetic parameter  $D$  without constraining the value of the coupling constant  $\lambda$  and thus, when possible, also at the critical point. For the case  $D = 0$  the phase transition appears when the coupling reaches the critical value  $\lambda_{\text{crit}} = \sqrt{\omega_a \omega_b}/2$ . In this case the QFI for  $D$  diverges as

$$H(D = 0) \sim \frac{\omega_b}{8\omega_a(\lambda - \lambda_{\text{crit}})^2}, \quad (7)$$

and the homodyne and the photon counting measurements both saturate the QFI in this limit, as shown in Fig. 2 (left panel). If  $D$  approaches the TRK value  $D \simeq D_{\text{TRK}}$  [cf. Eq. (3)], the phase transition is suppressed and there is no criticality in the system. The QFI for the two-mode state (for any value of  $\lambda$ ) reads

$$H(D_{\text{TRK}}) = \frac{2}{\omega_a^2} - \frac{16\lambda^2 \omega_a \omega_b}{(4\lambda^2 \omega_a + \omega_b (\omega_a + \omega_b))^2}. \quad (8)$$

$H(D_{\text{TRK}})$  is clearly higher for small frequencies of the radiation mode, whereas it decreases in the case of high frequencies. With respect to  $\lambda$ ,  $H(D_{\text{TRK}})$  has a minimum at  $\lambda^2 = \omega_b(\omega_a + \omega_b)^2/4\omega_a$  and the asymptotic value  $2/\omega_a^2$  for large and small  $\lambda$ . The ratio between the FI for the two measurements and the QFI is shown in Fig. 3 as a function of  $\lambda$  and  $\omega_a$ . One can also verify that the expansion in Eq. (6) is still valid also for larger values of  $\lambda$ , implying that homodyne

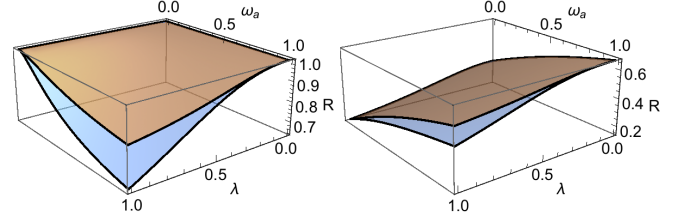


FIG. 3. Left: Ratio  $R = F^{(\text{hd})}(D_{\text{TRK}})/H(D_{\text{TRK}})$  (blue) and  $R = F^{(\text{hd})}(D_{\text{TRK}})/H_a(D_{\text{TRK}})$  (orange) for the homodyne detection when  $D$  assumes the TRK value, with  $\omega_b = 1$ . Right: the same ratios for the photon counting. Homodyne detection is optimal when  $\lambda$  and  $\omega_a$  are small. Photon counting, on the other hand, reaches optimality for large values of  $\omega_a$  and vanishing  $\lambda$ .

would be an excellent measurement strategy in most experimentally relevant situations. For example, setting  $D = D_{\text{TRK}}$  and  $\omega_a = \omega_b = 2\lambda$ , which corresponds to a remarkably high coupling constant, we still get a ratio of  $81/92 \simeq 0.88$ , while with the approximation of Eq. (6) we obtain  $7/8 \simeq 0.87$ .

In general, in the vicinity of the critical point  $D_{\text{crit}}$ , the asymptotic behavior of the two-mode QFI is

$$H(D) \underset{D \rightarrow D_{\text{crit}}}{\sim} \frac{1}{8(D - D_{\text{crit}})^2}, \quad (9)$$

that is, the QFI diverges, meaning that the amount of information that can be extracted increases enormously. This is another confirmation of the role of criticality in the enhancement of estimation [36, 38, 39].

The QFI for the reduced state of one of the two modes saturates the two-mode QFI  $H(D)$  when the system is close to the critical point. This is an interesting result: optimal estimation of  $D$  around the region of criticality can be achieved by measuring only a part of the system. Moreover, optimal parameter estimation can effectively be achieved with feasible experiments such as homodyne detection or photon counting. The FI for the  $x$ -quadrature measurement indeed saturates the QFI as  $D$  gets close to the critical value  $D_{\text{crit}}$ :

$$\frac{F^{(\text{hd})}(D)}{H(D)} \sim 1 - \frac{16\lambda^2 \omega_a^{3/2}}{4\lambda^2 \omega_a \omega_b + \omega_b^4} (D - D_{\text{crit}})^{1/2}. \quad (10)$$

We further find numerically that the photon counting measurements also saturates the QFI near the critical point (cf. Fig. 2, right panel).

*Results: Quantum discrimination.* We finally tackle the problem of discriminating between the two values of  $D$  that are most argued in recent literature:  $D = 0$  and  $D_{\text{TRK}}$ . By making a measurement on a subsystem, typically the cavity field, we want to decide which of the two hypotheses is correct. Quantum mechanics poses a limit to the discriminating ability, quantified by the Helstrom bound [30, 31]: if we label  $\rho^{(0)}$  and  $\rho^{(\text{TRK})}$ , respectively, the ground state in the two hypotheses, the lowest probability of error in the discrimination between these two states of the system is  $P_e = \frac{1}{2} [1 - \mathbb{D}(\rho^{(0)}, \rho^{(\text{TRK})})]$ , where  $\mathbb{D}(\rho^{(0)}, \rho^{(\text{TRK})})$  is the trace distance between the two states. The

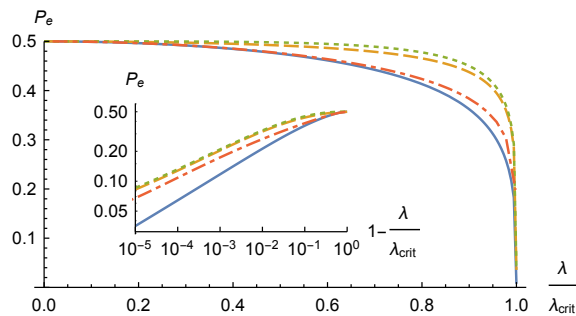


FIG. 4. The probabilities of error  $P_e$ , given by the Helstrom bound on the two-mode system (solid blue),  $P_e^{(a)}$ , for the photon mode (dot-dashed orange),  $P_e^{(\text{hd})}$  for homodyne detection (dashed yellow) and  $P_e^{(\text{pc})}$  for photon counting (dotted green) as functions of  $\lambda/\lambda_{\text{crit}}$ , with  $\omega_a = \omega_b = 1$ . In the inset, a log-log plot of the same quantities as  $\lambda$  approaches  $\lambda_{\text{crit}}$ . The probability of error is close to 1/2 for small  $\lambda$ , vanishing when  $\lambda \rightarrow \lambda_{\text{crit}}$ , i.e. when, for  $D = 0$ , the system is close to the quantum phase transition. The Helstrom bound on the mode  $a$  behaves differently from the two-mode bound near the critical value. The two proposed discrimination schemes, although not saturating the single-mode bound, have the same behavior in the limit  $\lambda \rightarrow \lambda_{\text{crit}}$ .

Helstrom bound is based on the assumption that the system has the same probability to be in either of the two states, reflecting the lack of any *a priori* information on which hypothesis is the correct one. The Helstrom bound calculated on the two-mode state can be only used as a benchmark for practical discrimination strategies, as the measurement that saturates it is a collective measurement on the two modes, not feasible in practice.

A more relevant benchmark is given by the Helstrom bound calculated on the reduced state of the mode  $a$ , i.e. in the discrimination between  $\rho_a^{(0)}$  and  $\rho_a^{(\text{TRK})}$ . Being these states mixed, the trace distance cannot be computed analytically. A diagonalization of the density operators expanded on a truncated Fock basis is required. The ensuing bound on the probability of error,  $P_e^{(a)}$ , is less stringent than the two-mode bound.

We show the dependence of  $P_e$  and  $P_e^{(a)}$  on  $\lambda/\lambda_c$  in Fig. 4: the probability of error is close to 1/2 for small  $\lambda$  and vanishes when  $\lambda$  reaches its critical value  $\lambda_c = \sqrt{\omega_a \omega_b}/2$  in the case  $D = 0$ . The dependence on  $\lambda$  in the neighborhood of  $\lambda_c$  is  $P_e \sim (\lambda_c - \lambda)^{1/4}$ . For  $P_e^{(a)}$  a numerical fit shows an exponent around 1/5. Thus we find that the discrimination between the two hypotheses is hard in the regime of small coupling, while criticality allows for a great improvement, should the optimal strategy be found.

To this end, we checked the performance of two feasible discrimination strategies using either the  $\hat{x}(0)$  quadrature measurement or photon counting on the mode  $a$ . The former exploits the fact that the probability distribution of the outcome of the quadrature measurement is a Gaussian with variance  $\sigma_{11}$ . In the case  $D = 0$ , when  $\lambda \rightarrow \lambda_{\text{crit}}$ ,  $\sigma_{11} \sim (\lambda_{\text{crit}} - \lambda)^{-1/2}$ . On the other hand, for  $D = \lambda^2/\omega_b$ ,  $\sigma_{11}$  does not depart much from its limit for  $\lambda \rightarrow 0$ , which is 1/2. Thus, close to the critical value, the Gaussian distribution for  $D = \lambda^2/\omega_b$  is very

narrow compared to the distribution for  $D = 0$ .

We can thus set up a readily feasible discrimination experiment as follows: if the outcome of the experiment is  $|x| < 2\sigma_{11}^{(\text{TRK})}$  [40] then the state of the system is  $\rho^{(\text{TRK})}$ , otherwise it is  $\rho^{(0)}$ . The corresponding probability of error is thus given by

$$P_e^{(\text{hd})} = \int_0^{2\sigma_{11}^{(\text{TRK})}} \mathcal{N}(0, \sigma_{11}^{(0)}) dx + \int_{2\sigma_{11}^{(\text{TRK})}}^{\infty} \mathcal{N}(0, \sigma_{11}^{(\text{TRK})}) dx, \quad (11)$$

where the first (second) term is the probability of detecting  $\rho^{(0)}$  ( $\rho^{(\text{TRK})}$ ) when the actual state was  $\rho^{(\text{TRK})}$  ( $\rho^{(0)}$ ), and  $\mathcal{N}(\mu, \sigma)$  is the normal distribution with mean  $\mu$  and variance  $\sigma$ .

In a photon counting experiment, we can exploit the fact that, when  $D = 0$ , the average photon number diverges near the phase transition [36], while it is close to zero if the phase transition is suppressed by the presence of the  $A^2$  term. Thus, we can discriminate between the two hypotheses by setting a threshold photon number  $n_T$  and assigning any outcome below that threshold to the hypothesis  $\rho^{(\text{TRK})}$  and any outcome above to  $\rho^{(0)}$ . The probability of error in this case would be

$$P_e^{(\text{pc})} = \frac{1}{2} \left( \sum_{n=0}^{n_T} p_0(n) + 1 - \sum_{n=0}^{n_T} p_{\text{TRK}}(n) \right). \quad (12)$$

We find the optimal threshold value is  $n_T = 0$ , i.e. the discrimination is between no photons and any number of photons. This is a harder question to settle in a realistic experiment.

The resulting  $P_e^{(\text{hd})}$  and  $P_e^{(\text{pc})}$  are compared to the Helstrom bounds in Fig. 4. We see that the homodyne scheme is slightly better than the photon counting one. Interestingly, these two feasible discrimination schemes have the same behavior as the Helstrom bound  $P_e^{(a)}$  on the reduced state when approaching the critical point, although neither of them are optimal.

Before closing the Letter, we would like to comment on the feasibility of the proposed measurements, which require access to the cavity mode  $a$  (see Fig. 1). One possible way to access the intra-cavity field is to suddenly switch off the coupling  $\lambda$ , a drastic yet experimentally feasible procedure [1]. Allowing one of the cavity mirrors to have a small but finite transmissivity, one may subsequently collect the cavity output field (i.e. the radiation that gradually leaks out into the external world). In absence of light-matter coupling and other loss mechanisms, the cavity output field can be used to extract the full quantum statistics of mode  $a$  just before the switch-off [41].

*Discussion.* In conclusion, we have discussed the detection of the diamagnetic term in a generalized Dicke model of light-matter interaction, formulating the problem in terms of quantum parameter estimation or discrimination between two alternatives. In both cases we discussed the performance of two feasible measurements, homodyne and photon counting, that allow for the extraction of a large fraction of the available information: this fraction becomes optimal in some experimentally relevant regimes, such as the small-coupling regime. In future studies, the ideas presented in this letter may be generalised to test the validity of alternative or more complex models of light-matter interaction.

This work has been supported by EU through the Erasmus+ Placement programme, the Marie Skłodowska-Curie Action H2020-MSCA-IF-2015 (project ConAQuMe) and the collaborative Project QuProCS (Grant Agreement 641277), the EPSRC UK (grant No. EP/K026267/1), the European Research Council (ERC StG QQCOP, Grant No. 637352), the Royal Society (Grant No. IE150570), and by UniMI through the H2020 Transition Grant 15-6-3008000-625.

- 
- [1] G. Günter, A. A. Anappara, J. Hees, A. Sell, G. Biasiol, L. Sorba, S. De Liberato, C. Ciuti, A. Tredicucci, A. Leitenstorfer, and R. Huber, *Nature* **458**, 178 (2009).
- [2] C. Maissen, G. Scalari, F. Valmorra, M. Beck, J. Faist, S. Cibella, R. Leoni, C. Reichl, C. Charpentier, and W. Wegscheider, *Phys. Rev. B* **90**, 205309 (2014).
- [3] C. Ciuti, G. Bastard, and I. Carusotto, *Phys. Rev. B* **72**, 115303 (2005).
- [4] S. De Liberato, C. Ciuti, and I. Carusotto, *Phys. Rev. Lett.* **98**, 103602 (2007).
- [5] P. Nataf and C. Ciuti, *Nat. Commun.* **1**, 72 (2010).
- [6] C. Emary and T. Brandes, *Phys. Rev. A* **69**, 053804 (2004).
- [7] C. Cohen-Tannoudji, J. Dupont-Roc, and G. Grynberg, *Photons and Atoms* (Wiley-VCH Verlag GmbH, Weinheim, Germany, 1997).
- [8] I. Bialynicki-Birula and K. Rzażewski, *Phys. Rev. A* **19**, 301 (1979).
- [9] K. Rzażewski and K. Wódkiewicz, *Phys. Rev. A* **43**, 593 (1991).
- [10] M. Bamba and T. Ogawa, *Phys. Rev. A* **90**, 063825 (2014).
- [11] L. Chirolli, M. Polini, V. Giovannetti, and A. H. MacDonald, *Phys. Rev. Lett.* **109**, 267404 (2012).
- [12] S. De Liberato, *Phys. Rev. Lett.* **112**, 016401 (2014).
- [13] A. Vukics, T. Griebner, and P. Domokos, *Phys. Rev. Lett.* **112**, 073601 (2014).
- [14] A. Vukics and P. Domokos, *Phys. Rev. A* **86**, 053807 (2012).
- [15] J. Keeling, *J. Phys.: Condens. Matter* **19**, 295213 (2007).
- [16] O. Viehmann, J. von Delft, and F. Marquardt, *Phys. Rev. Lett.* **107**, 113602 (2011).
- [17] C. Ciuti and P. Nataf, *Phys. Rev. Lett.* **109**, 179301 (2012); O. Viehmann, J. von Delft, and F. Marquardt, "Reply to Comment on "Superradiant Phase Transitions and the Standard Description of Circuit QED"," (2012), arXiv:1202.2916.
- [18] T. Jaako, Z.-L. Xiang, J. J. Garcia-Ripoll, and P. Rabl, "Inhibition of ground-state superradiance and light-matter decoupling in circuit QED," (2016), arXiv:1602.05756.
- [19] J. J. García-Ripoll, B. Peropadre, and S. De Liberato, *Sci. Rep.* **5**, 16055 (2015).
- [20] S. L. Braunstein and C. M. Caves, *Phys. Rev. Lett.* **72**, 3439 (1994).
- [21] M. G. A. Paris, J. Rehacek (Eds), *Quantum State Estimation*, Lect. Notes Phys., Vol. 649 (Springer, Berlin, 2004).
- [22] S. Amari and H. Nagaoka, *Methods of Information Geometry* (American Mathematical Society, 2007).
- [23] B. M. Escher, R. L. de Matos Filho, and L. Davidovich, *Nature Phys.* **7**, 406 (2011).
- [24] D. C. Brody and L. P. Hughston, *Proc. Royal Soc. A* **454**, 2445 (1998).
- [25] M. G. A. Paris, *Int. J. Quantum Inf.* **7**, 125 (2009).
- [26] A. A. Anappara, S. De Liberato, A. Tredicucci, C. Ciuti, G. Biasiol, L. Sorba, and F. Beltram, *Phys. Rev. B* **79**, 201303 (2009).
- [27] T. Niemczyk, F. Deppe, H. Huebl, E. Menzel, F. Hocke, M. Schwarz, J. Garcia-Ripoll, D. Zueco, T. Hümmer, E. Solano, *et al.*, *Nature Physics* **6**, 772 (2010).
- [28] P. Forn-Díaz, J. Lisenfeld, D. Marcos, J. J. García-Ripoll, E. Solano, C. J. P. M. Harmans, and J. E. Mooij, *Phys. Rev. Lett.* **105**, 237001 (2010).
- [29] T. Tufarelli, K. R. McEney, S. A. Maier, and M. S. Kim, *Phys. Rev. A* **91**, 063840 (2015).
- [30] C. W. Helstrom, *Quantum detection and estimation theory* (Academic Press New York, 1976).
- [31] J. A. Bergou, *J. Mod. Opt.* **57**, 160 (2010).
- [32] See Supplemental Material at [URL will be inserted by publisher].
- [33] H. Cramér, *Mathematical Methods of Statistics* (Princeton Univ. Press, Princeton, 1946).
- [34] A. Monras, "Phase space formalism for quantum estimation of Gaussian states," (2013), arXiv:1303.3682.
- [35] Z. Jiang, *Phys. Rev. A* **89**, 032128 (2014).
- [36] M. Bina, I. Amelio, and M. G. A. Paris, *Phys. Rev. E*, in press (2016), arXiv:1601.04015.
- [37] P. Marian and T. A. Marian, *Phys. Rev. A* **86**, 022340 (2012).
- [38] P. Zanardi, P. Giorda, and M. Cozzini, *Phys. Rev. Lett.* **99**, 100603 (2007).
- [39] P. Zanardi, M. G. A. Paris, and L. Campos Venuti, *Phys. Rev. A* **78**, 042105 (2008).
- [40] The choice of  $2\sigma_{11}^{(\text{TRK})}$  here is arbitrary. The optimal threshold value depends on the parameters of the problem. Even by optimizing over this parameter we do not saturate the Helstrom bound.
- [41] C. Gardiner and P. Zoller, *Quantum Noise: A Handbook of Markovian and Non-Markovian Quantum Stochastic Methods with Applications to Quantum Optics*, Springer Series in Synergetics (Springer, 2004).

**SUPPLEMENTAL MATERIAL**

**Covariance matrix of the ground state**

As is shown in [29], the USC Hamiltonian in Eq. (1) of the paper can be cast to the diagonal form of Eq. (2), where the frequencies  $\omega_U, \omega_L$  are

$$\omega_{U,L}^2 = \frac{\omega_a^2 + 4D\omega_a + \omega_b^2}{2} \pm \sqrt{\left(\frac{\omega_a^2 + 4D\omega_a - \omega_b^2}{2}\right)^2 + 4\lambda^2\omega_a\omega_b}. \quad (\text{A.1})$$

The symplectic matrix that transforms the vector  $(a, b, a^\dagger, b^\dagger)$  of the original-mode creation and annihilation operators into the vector of polaritonic modes  $(p_U, p_L, p_U^\dagger, p_L^\dagger)$ , is given by

$$\bar{S} = \begin{pmatrix} \cos\theta f_+ \left(\frac{\omega_U}{\omega_a}\right) - \sin\theta f_+ \left(\frac{\omega_U}{\omega_b}\right) & \cos\theta f_- \left(\frac{\omega_U}{\omega_a}\right) - \sin\theta f_- \left(\frac{\omega_U}{\omega_b}\right) \\ \sin\theta f_+ \left(\frac{\omega_L}{\omega_a}\right) + \cos\theta f_+ \left(\frac{\omega_L}{\omega_b}\right) & \sin\theta f_- \left(\frac{\omega_L}{\omega_a}\right) + \cos\theta f_- \left(\frac{\omega_L}{\omega_b}\right) \\ \cos\theta f_- \left(\frac{\omega_U}{\omega_a}\right) - \sin\theta f_- \left(\frac{\omega_U}{\omega_b}\right) & \cos\theta f_+ \left(\frac{\omega_U}{\omega_a}\right) - \sin\theta f_+ \left(\frac{\omega_U}{\omega_b}\right) \\ \sin\theta f_- \left(\frac{\omega_L}{\omega_a}\right) + \cos\theta f_- \left(\frac{\omega_L}{\omega_b}\right) & \sin\theta f_+ \left(\frac{\omega_L}{\omega_a}\right) + \cos\theta f_+ \left(\frac{\omega_L}{\omega_b}\right) \end{pmatrix} \quad (\text{A.2})$$

where

$$\cos 2\theta = \frac{\omega_a^2 + 4D\omega_a - \omega_b^2}{\omega_U^2 - \omega_L^2} \quad \sin(2\theta) = -\frac{4\lambda\sqrt{\omega_a\omega_b}}{\omega_U^2 - \omega_L^2}. \quad (\text{A.3})$$

and we define

$$f_\pm(x) = \frac{1}{2} \left( \sqrt{x} \pm \frac{1}{\sqrt{x}} \right). \quad (\text{A.4})$$

The ground state of the diagonalized Hamiltonian is the vacuum, i.e. a Gaussian state with no displacement and a covariance matrix  $\sigma_0 = \mathbb{I}/2$  in the basis of the quadratures  $x_{U,L} = (p_{U,L} + p_{U,L}^\dagger)/\sqrt{2}$ ,  $y_{U,L} = -i(p_{U,L} - p_{U,L}^\dagger)/\sqrt{2}$ .

To obtain the covariance matrix  $\sigma$  in the original modes  $a$  and  $b$ , transform  $\sigma_0$  using a symplectic matrix  $S$  that can easily be obtained from  $\bar{S}$ . After some simplifications, we have

$$\sigma = S\sigma_0S^T = \begin{pmatrix} \frac{\omega_a(\omega_b^2 + \omega_L\omega_U)}{\omega_L\omega_U(\omega_L + \omega_U)} & 0 & -\frac{2\lambda\omega_a\omega_b}{\omega_L\omega_U(\omega_L + \omega_U)} & 0 \\ 0 & \frac{2(\omega_a^2 + 4d\omega_a + \omega_L\omega_U)}{2\omega_a\omega_L + 2\omega_a\omega_U} & 0 & \frac{2\lambda}{\omega_L + \omega_U} \\ -\frac{2\lambda\omega_a\omega_b}{\omega_L\omega_U(\omega_L + \omega_U)} & 0 & \frac{\omega_b(\omega_a^2 + 4d\omega_a + \omega_L\omega_U)}{\omega_L\omega_U(\omega_L + \omega_U)} & 0 \\ 0 & \frac{2\lambda}{\omega_L + \omega_U} & 0 & \frac{\omega_b^2 + \omega_L\omega_U}{\omega_b(\omega_L + \omega_U)} \end{pmatrix} \quad (\text{A.5})$$

**Quantum Fisher information and Fisher information for homodyne detection and photon counting**

*QFI for the two-mode state*

Given  $\sigma$ , we can calculate the quantum Fisher information (QFI) using Eq. (5) of the paper. If the state is pure, the solution of Eq. (6) is  $\Phi = -\partial\sigma$ . This in turn yields the following expression for the QFI:

$$H(D) = 2(\partial\sigma_{1,1}\partial\sigma_{2,2} + 2\partial\sigma_{2,4}\partial\sigma_{3,1} + \partial\sigma_{3,3}\partial\sigma_{4,4}). \quad (\text{A.6})$$

Here we report the general expression of the QFI (after some manipulations). The relevant cases are discussed in the paper.

$$H = \frac{2\omega_a^2\omega_b^2}{\omega_L^4\omega_U^4(\omega_L + \omega_U)^4} \left\{ (\omega_b^2 [16d^2\omega_a^2 + 8d\omega_a(\omega_a^2 + 3\omega_b^2 + 2\omega_L\omega_U)] + \omega_a^4 + 4\omega_L\omega_U(\omega_a^2 + \omega_b^2) + 6\omega_a^2\omega_b^2 + \omega_b^4) \right. \\ \left. - 8\lambda^2\omega_a\omega_b(4d\omega_a + \omega_a^2 + 2\omega_b^2) + 32\lambda^4\omega_a^2 \right\}. \quad (\text{A.7})$$

*QFI for the reduced state of mode a*

The covariance matrix  $\sigma_a$  of the reduced state  $\rho_a$  of the photonic mode is simply the upper left diagonal block of  $\sigma$ . The corresponding state is a squeezed thermal state

$$\rho_a = S(r) \nu_{th} S^\dagger(r) = \frac{1}{1+N} \sum_m \left( \frac{N}{1+N} \right)^m S(r) |m\rangle \langle m| S^\dagger(r), \quad (\text{A.8})$$

where  $N$  is the number of thermal photons and  $r$  is the squeezing parameter:

$$N = \frac{1}{2} \left( \sqrt{\frac{(\omega_b^2 + \omega_L \omega_U)(4D\omega_a + \omega_a^2 + \omega_L \omega_U)}{\omega_L \omega_U (\omega_L + \omega_U)^2}} - 1 \right) \quad (\text{A.9})$$

$$r = \frac{1}{4} \log \frac{\omega_L \omega_U (4D\omega_a + \omega_a^2 + \omega_L \omega_U)}{\omega_a^2 (\omega_b^2 + \omega_L \omega_U)}. \quad (\text{A.10})$$

The QFI for the reduce state can be obtained easily by solving Eq. (6) of the paper for  $\Phi$ . Being  $\sigma_a$  diagonal, we simply find that  $\Phi$  is diagonal with

$$\Phi_{11} = 2 \frac{(\partial \sigma_a)_{11} + 4(\sigma_a)_{11}^2 (\partial \sigma_a)_{22}}{16(\sigma_a)_{11}^2 (\sigma_a)_{22}^2 - 1} \quad (\text{A.11})$$

$$\Phi_{22} = 2 \frac{(\partial \sigma_a)_{22} + 4(\sigma_a)_{22}^2 (\partial \sigma_a)_{11}}{16(\sigma_a)_{11}^2 (\sigma_a)_{22}^2 - 1}. \quad (\text{A.12})$$

The corresponding QFI is

$$H_a = \frac{4(2\sigma_{11}^2 (\partial \sigma_{22})^2 + 2\sigma_{22}^2 (\partial \sigma_{11})^2 + \partial \sigma_{11} \partial \sigma_{22})}{16\sigma_{11}^2 \sigma_{22}^2 - 1}. \quad (\text{A.13})$$

*Fisher information for the homodyne detection*

In a homodyne detection experiment one can measure the field mode quadrature at an arbitrary phase, i.e. the expected value of the operator  $\hat{x}(\phi) = (ae^{-i\phi} + a^\dagger e^{i\phi})/\sqrt{2}$ .

The probability density for the outcome of a homodyne measurement is easily obtained from the Wigner function of the reduced state of the photon mode  $\rho_a = \text{Tr}_b[\rho]$ , which is a Gaussian distribution with zero mean and covariance matrix  $\text{diag}(\sigma_{11}, \sigma_{22})$ .

The probability  $p_\phi(x)$  of the outcome  $x(\phi)$  for the measurement is the marginal distribution of the Wigner function, obtained after a rotation of an angle  $\phi$  in the phase space:

$$\begin{aligned} p_\phi(x) &= \int dy W[\rho_a](x \cos \phi - y \sin \phi, x \sin \phi + y \cos \phi) \\ &= \mathcal{N}(0, \sigma_{11} \cos^2 \phi + \sigma_{22} \sin^2 \phi), \end{aligned} \quad (\text{A.14})$$

that is, a normal distribution with variance  $\sigma_{11} \cos^2 \phi + \sigma_{22} \sin^2 \phi$ . The Fisher information (FI) for this distribution is easily obtained to be

$$F_\phi(D) = \int dx \frac{[\partial p_\phi(x)]^2}{p_\phi(x)} = \frac{(\partial \sigma_{11} \cos^2 \phi + \partial \sigma_{22} \sin^2 \phi)^2}{2(\sigma_{11} \cos^2 \phi + \sigma_{22} \sin^2 \phi)^2}. \quad (\text{A.15})$$

It is easy to check that the FI  $F_\phi(D)$  has maxima for  $\phi = 0, \pi/2$ , in which

$$F_0(D) = \frac{(\partial \sigma_{11})^2}{2\sigma_{11}}, \quad F_{\frac{\pi}{2}}(D) = \frac{(\partial \sigma_{22})^2}{2\sigma_{22}}. \quad (\text{A.16})$$

Numerical analysis indicates that  $F_0(D) \geq F_{\frac{\pi}{2}}(D)$ , thus  $\phi = 0$  is the optimal angle to perform the homodyne measurement.